Electronic Supplementary Information for

A self-phosphorized carbon-based monolithic chainmail electrode for high-current-density and durable alkaline water splitting

Shixiong Min,*[a,b,c] Zhe Meng,[a,b,c] Yaoyao Zhao,[a,b,c] Wenjing Li,[a,b,c] Zhengguo Zhang,[a,b,c] and Fang Wang[a,b,c]

[a] *School of Chemistry and Chemical Engineering, North Minzu University, Yinchuan, 750021, P. R. China. E-mail: sxmin@nun.edu.cn*

[b] *Ningxia Key Laboratory of Solar Chemical Conversion Technology, North Minzu University, Yinchuan 750021, P. R. China.*

[c] *Key Laboratory of Chemical Engineering and Technology, State Ethnic Affairs Commission, North Minzu University, Yinchuan, 750021, P. R. China.*

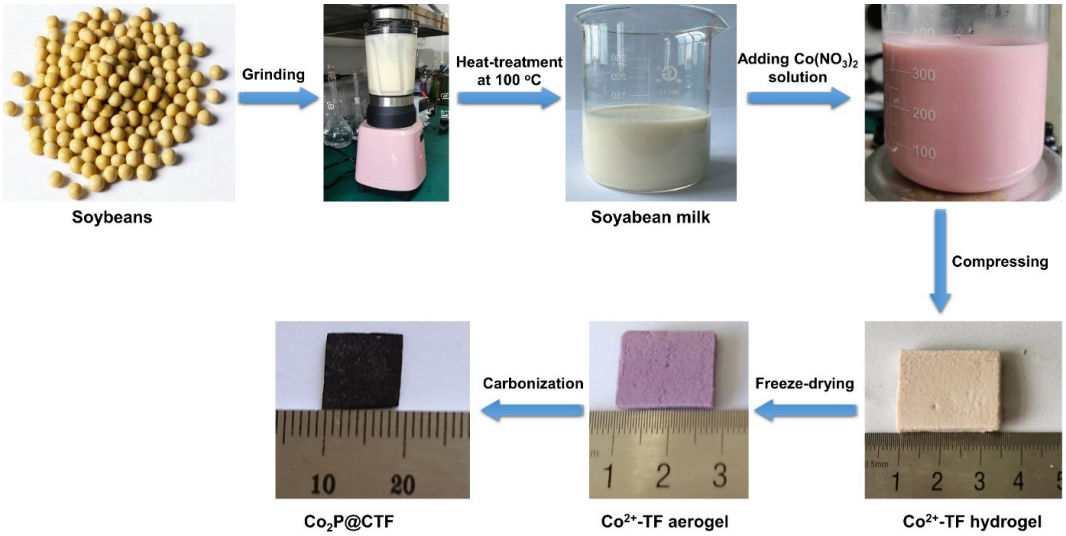

Fig. S1 Schematics of preparation of Co_2P@CTF monolithic chainmail electrode.

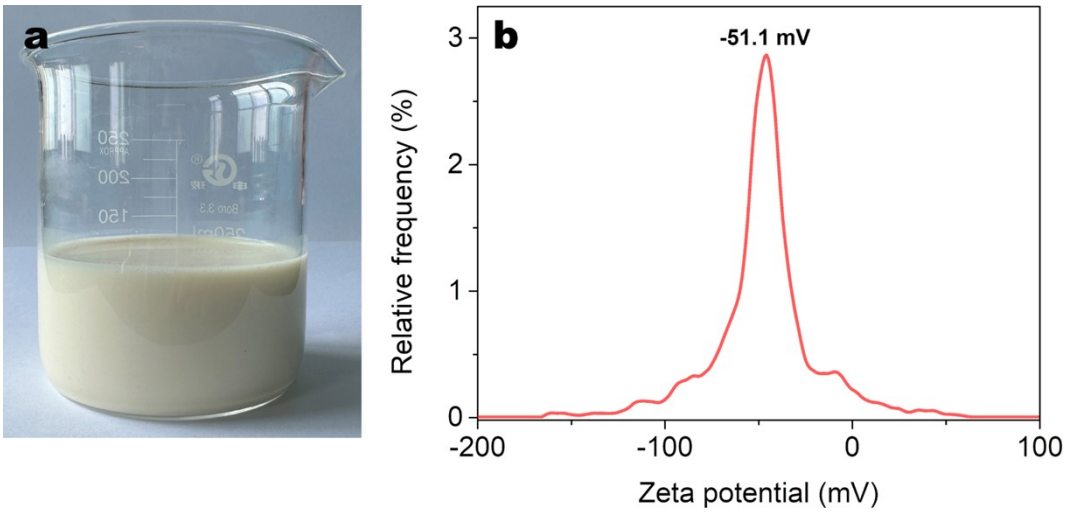

Fig. S2 (a) Photograph of denatured soybean protein suspension and (b) the corresponding Zeta potential.

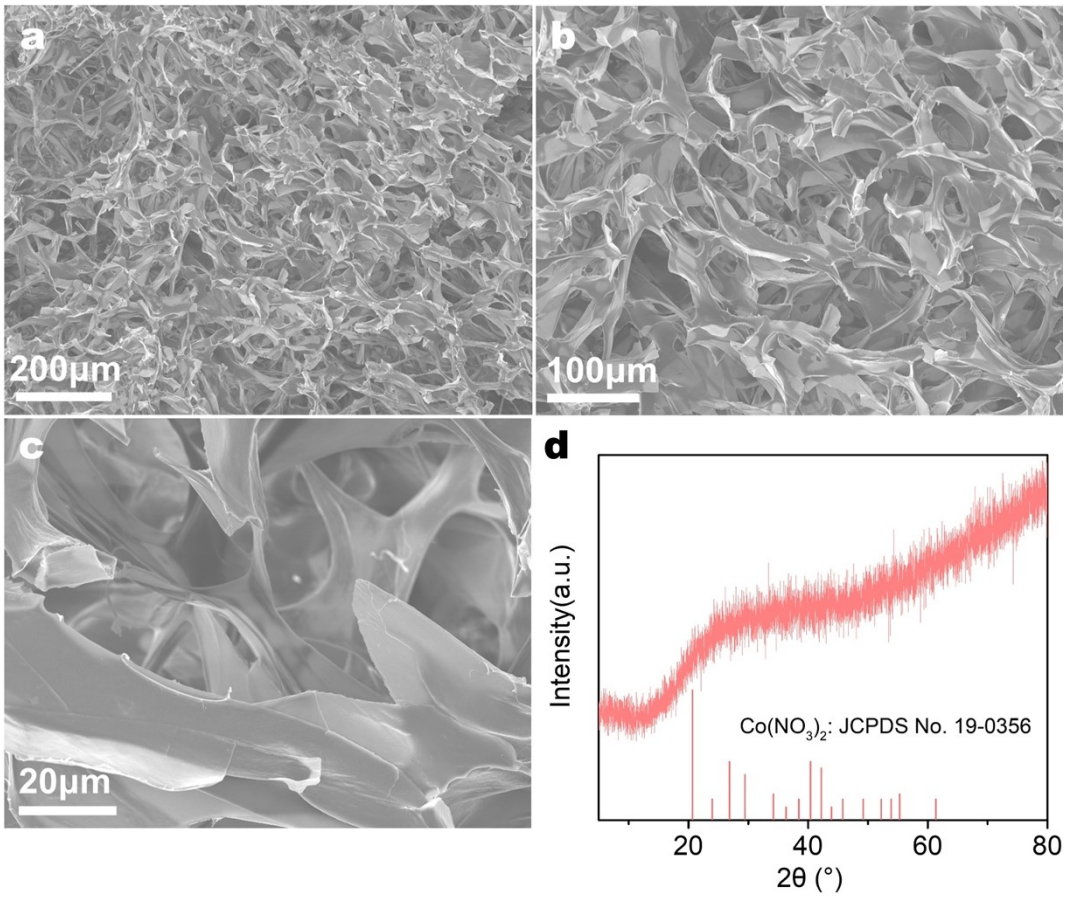

Fig. S3 (a-c) SEM images and (d) XRD pattern of Co^{2+}-TF aerogel.

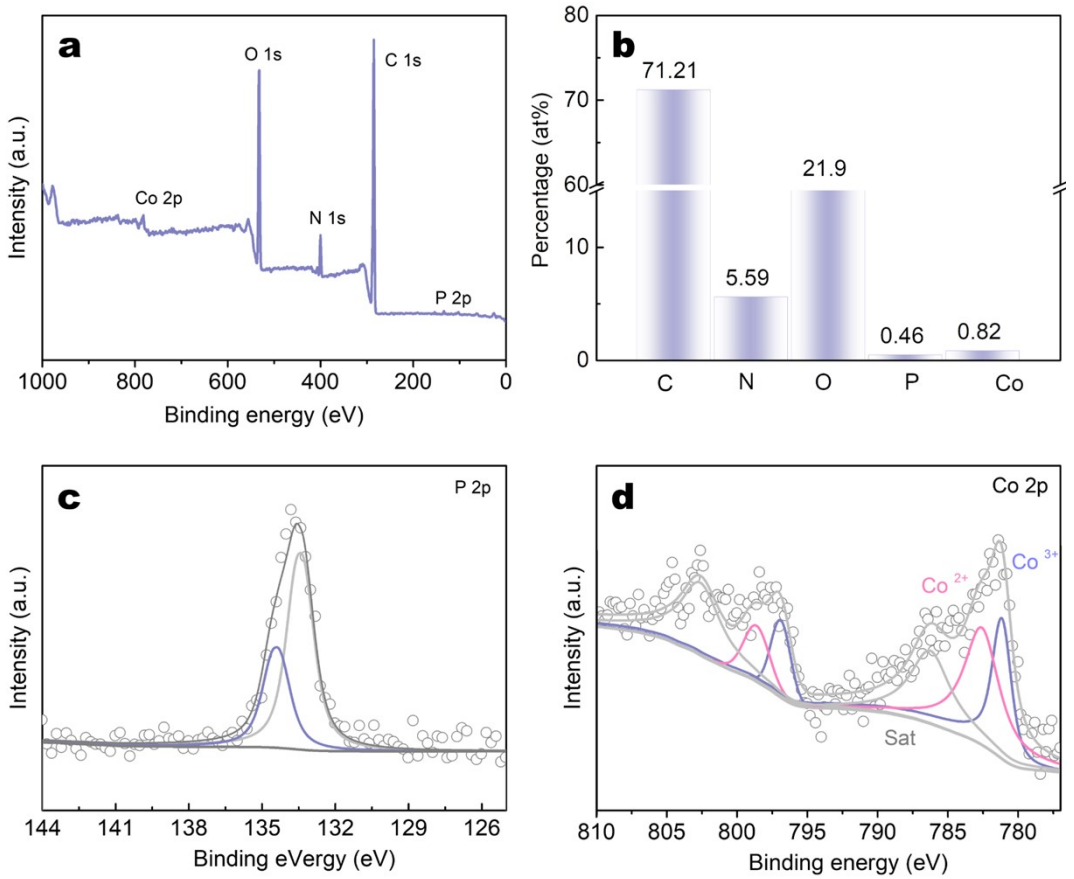

Fig. S4 (a) XPS survey spectrum of Co^{2+}-TF aerogel. (b) the contents of C, N, O, P and Co elements of Co^{2+}-TF aerogel. (c) P 2p and (d) Co 2p XPS spectra of Co^{2+}-TF aerogel.

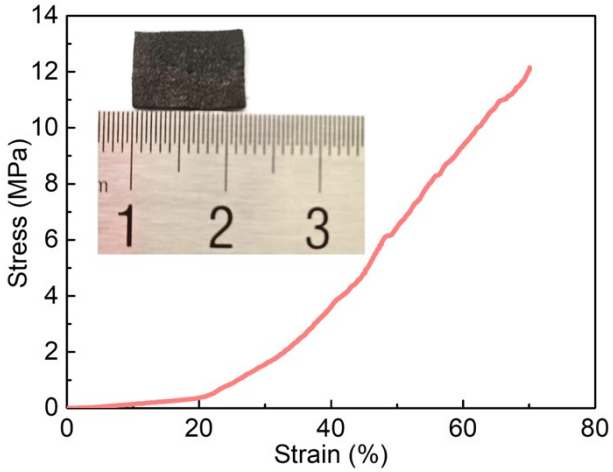

Fig. S5 Compressive-strain curve of Co_2P@CTF.

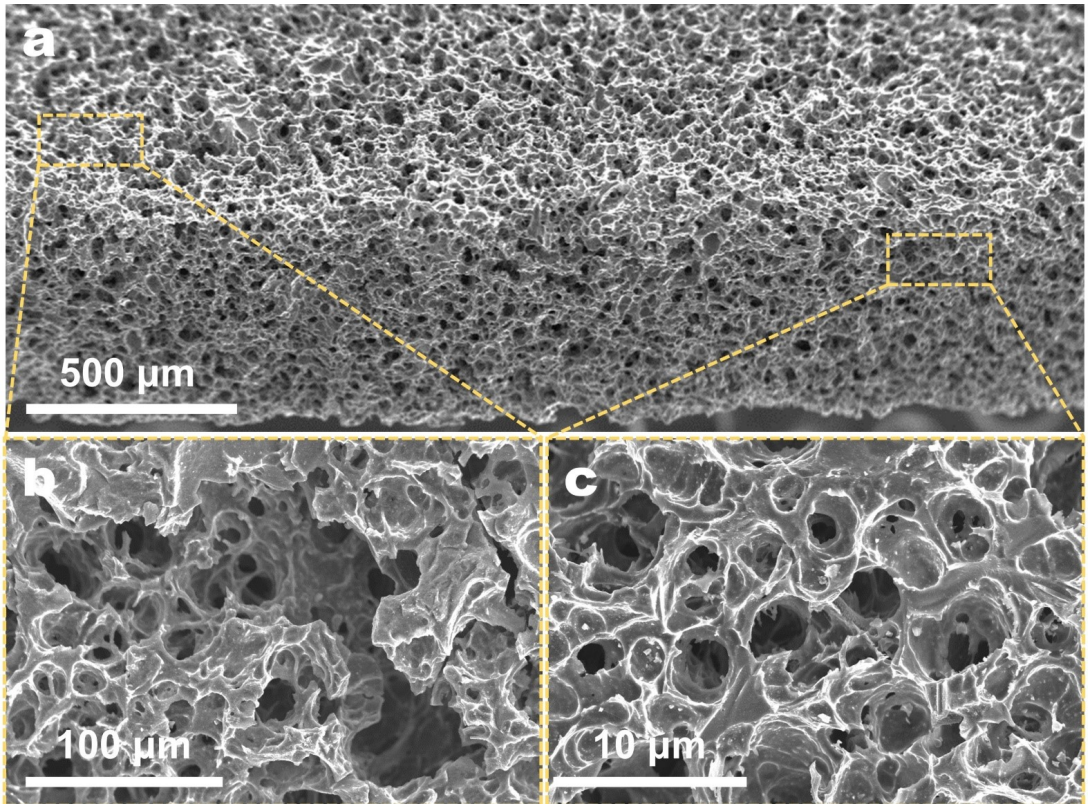

Fig. S6 SEM images of CTF electrode.

Table S1 ICP-OES analysis of Co_2P@CTF.

Element	Content (wt %)	Co/P ratio
Co	0.75	2.2:1
P	0.18	

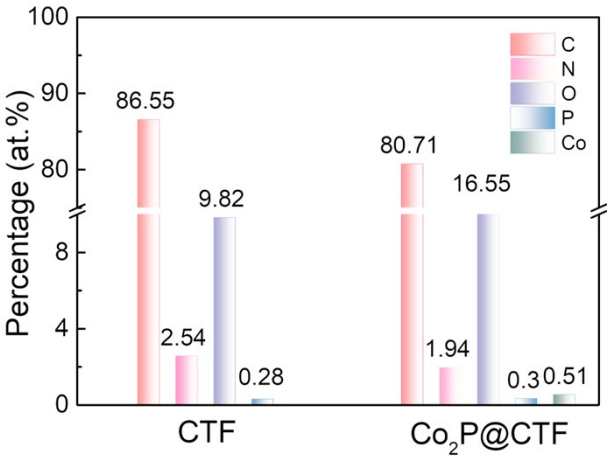

Fig. S7 The contents of C, N, O, P, and Co elements in CTF and Co_2P@CTF.

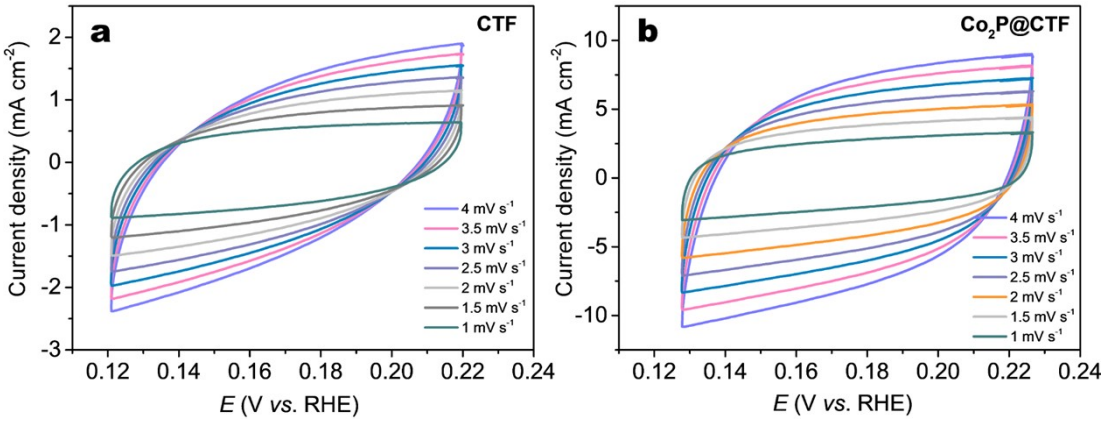

Fig. S8 CV curves of (a) CTF and (b) Co_2P@CTF electrode measured at the nonfaradaic potential region of 0.12 to 0.22 V vs. RHE over the scan rate from 1 to 4 mV s^{-1}.

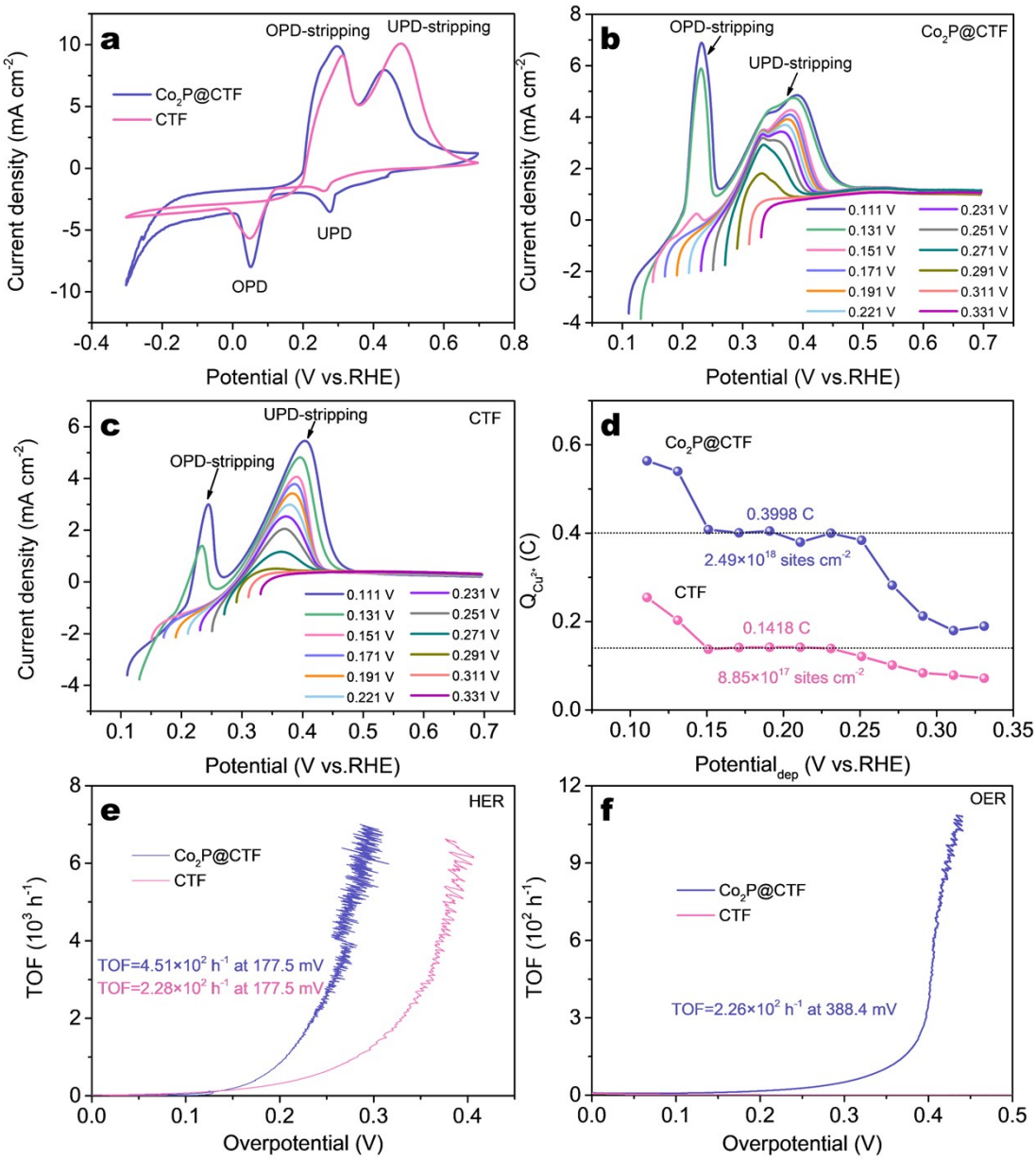

Fig. S9 (a) CV curves for Co_2P@CTF and CTF electrodes in a solution of 0.5 M H_2SO_4+20 mM $CuSO_4$+60 mM NaCl at a scan rate of 1 mV s^{-1}. LSV curves of (b) Co_2P@CTF and (c) CTF electrodes for the stripping of Cu deposited at different overpotentials from -0.111 to 0.331 V vs. RHE in a 0.5 M H_2SO_4+20 mM $CuSO_4$+60 mM NaCl solution (scan rate of 1 mV s^{-1}). (d) The charges required to strip the Cu deposited at different underpotentials for Co_2P@CTF and CTF electrodes. The dependence of TOF on overpotential for the (e) HER and (f) OER over the Co_2P@CTF and CTF electrodes.

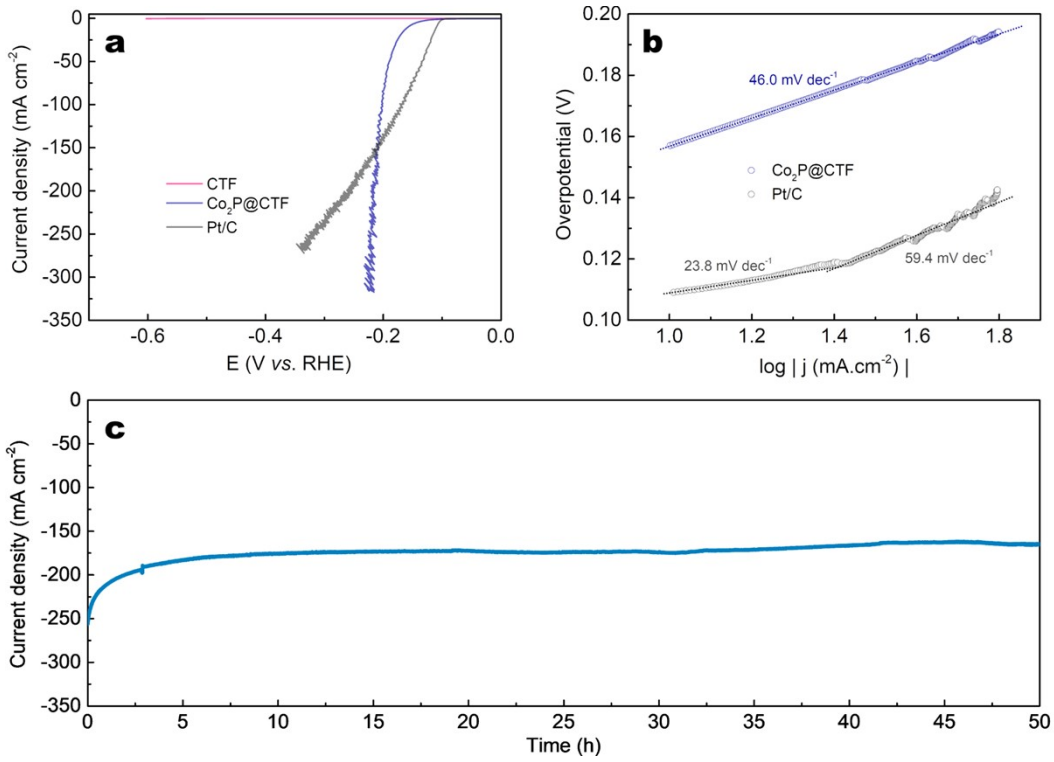

Fig. S10 (a) HER polarization curves of CTF, Co_2P@CTF, and Pt/C in 0.5 M H_2SO_4 at a scan rate of 0.5 mV s^{-1}. (b) Tafel plots of CTF, Co_2P@CTF, and Pt/C. (c) Long-term stability test of Co_2P@CTF electrode for HER in 0.5 M H_2SO_4.

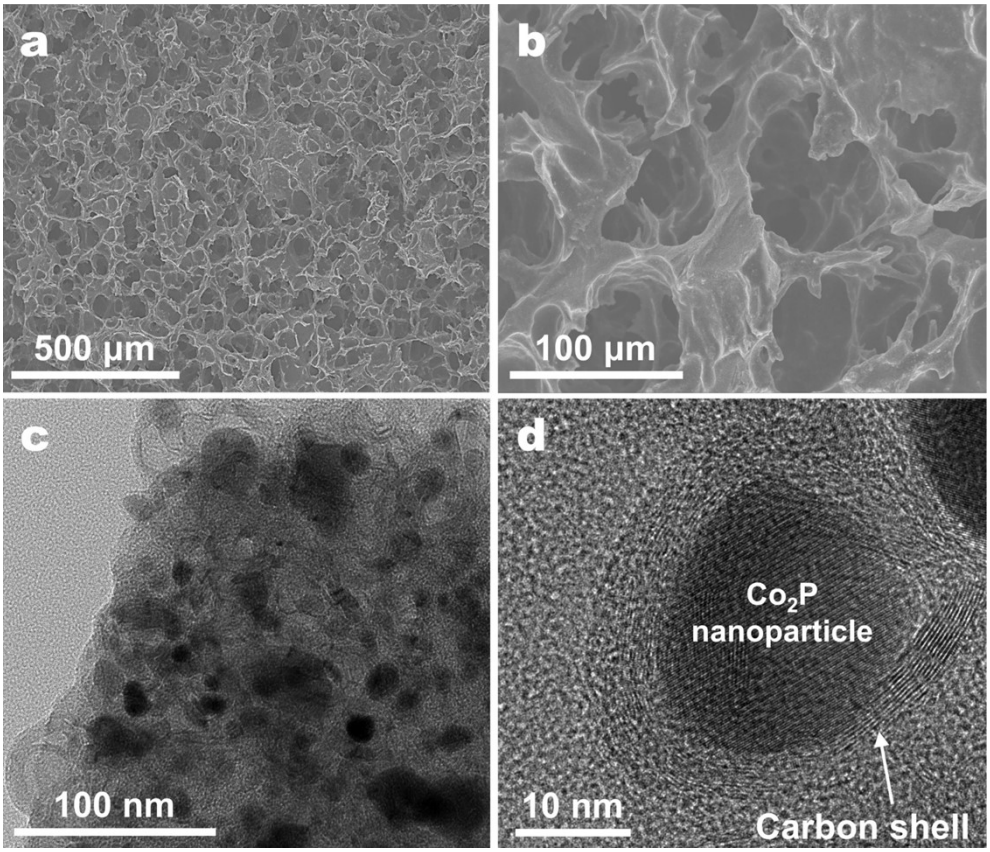

Fig. S11 (a and b) SEM and (c and d) TEM images of Co_2P@CTF electrode after HER stability test in 1.0 M KOH solution.

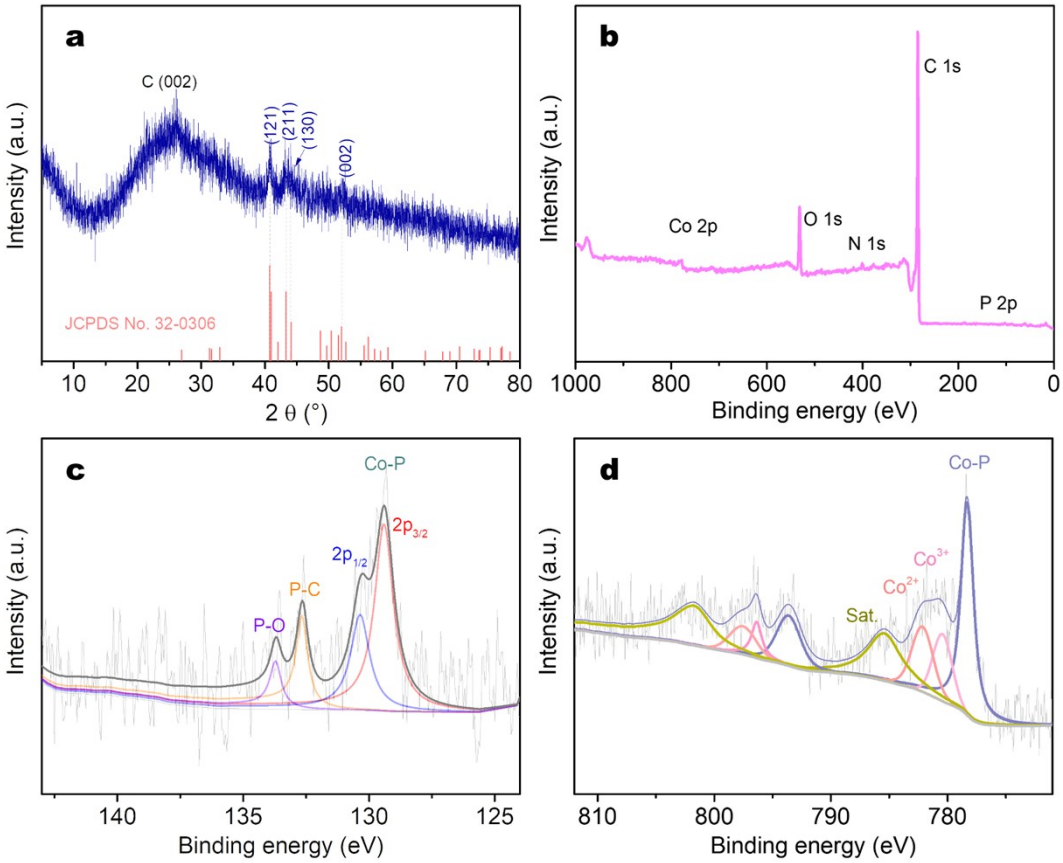

Fig. S12 (a) XRD pattern and (b) XPS survey spectrum, (c) P 2p, and (d) Co 2p XPS spectra of Co_2P@CTF electrode after HER stability test in 1.0 M KOH solution.

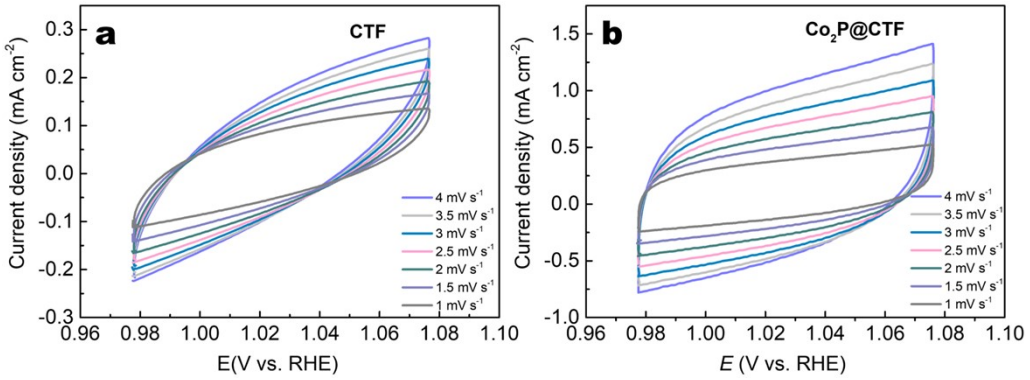

Fig. S13 CV curves of (a) CTF and (b) Co_2P@CTF electrode measured at the nonfaradaic potential region of 0.98 to 1.08 V *vs*. RHE over the scan rate from 1 to 4 mV s^{-1}.

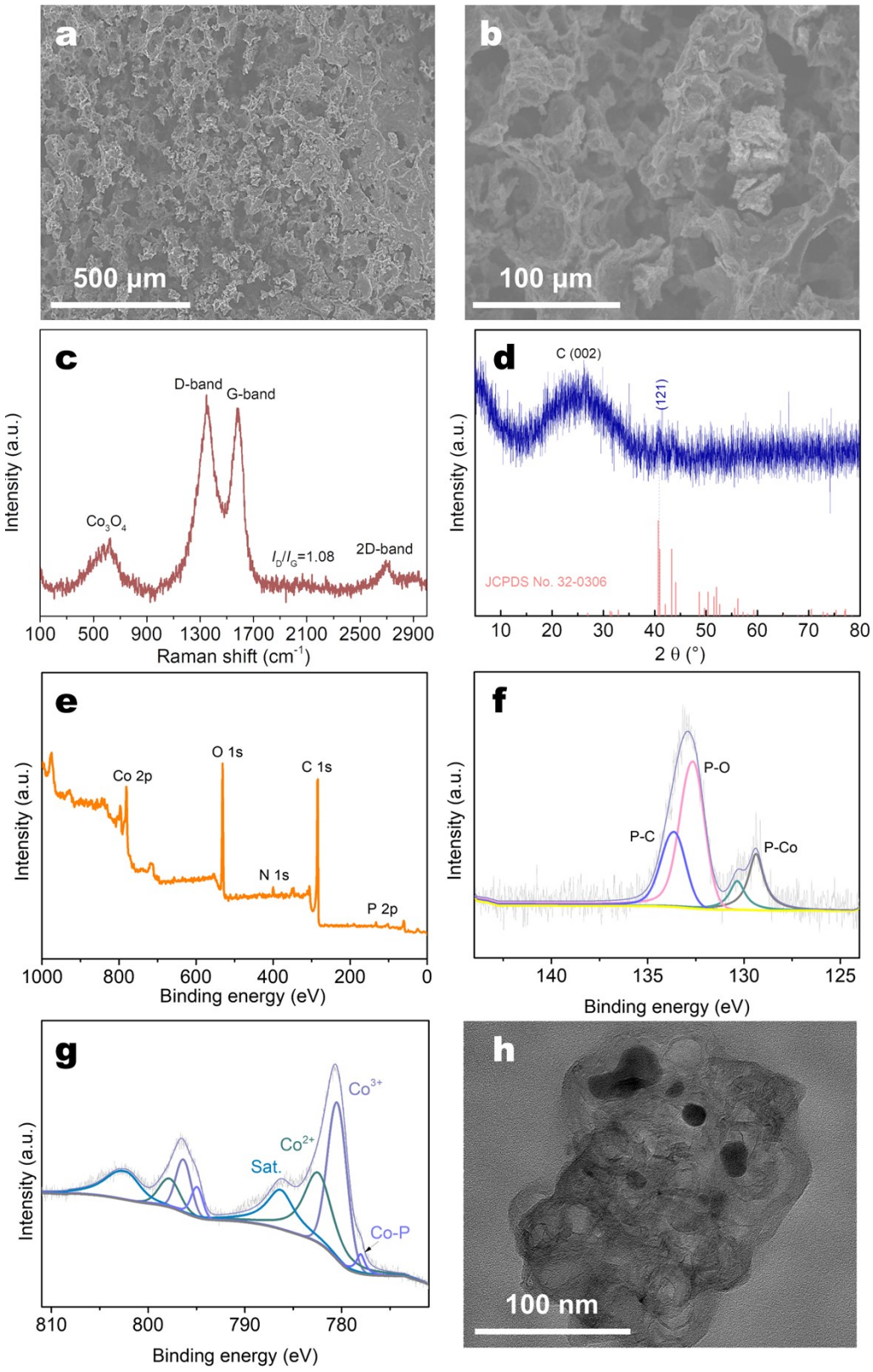

Fig. S14 (a and b) SEM images, (c) Raman spectrum, (d) XRD pattern, (e) XPS survey spectrum, (f) P 2p, (g) Co 2p XPS spectra, and (h) TEM image of Co_2P@CTF electrode after OER stability test in 1.0 M KOH solution.

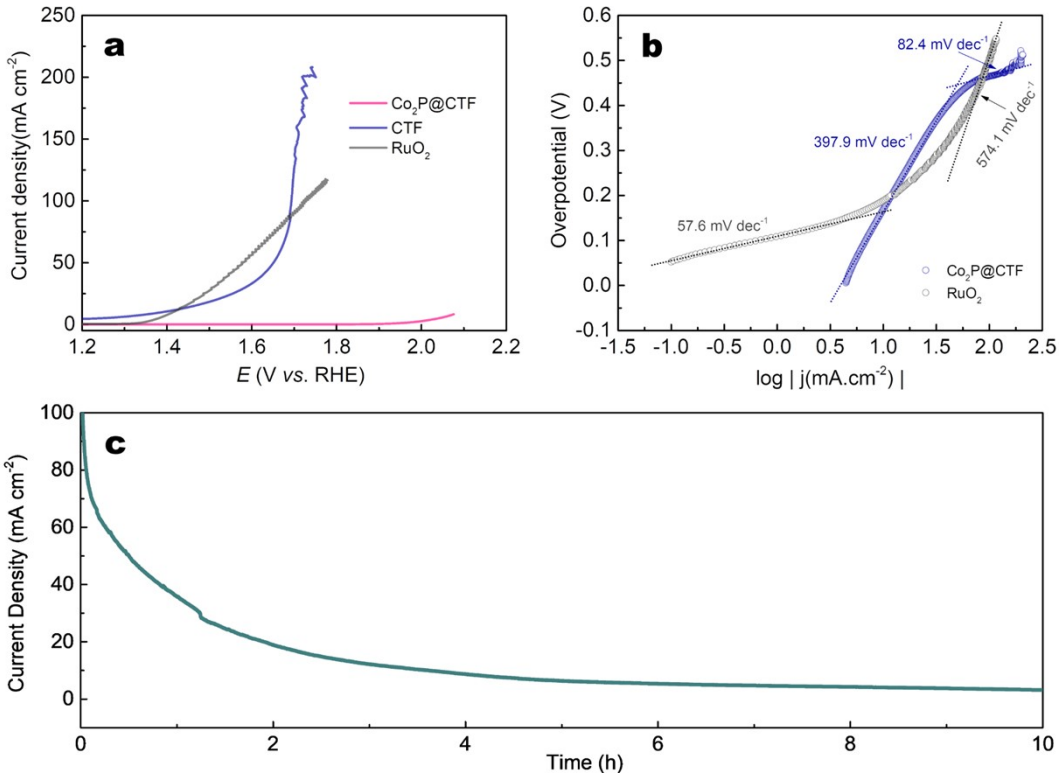

Fig. S15 (a) OER polarization curves of CTF, Co_2P@CTF, and Pt/C in 0.5 M H_2SO_4 at a scan rate of 0.5 mV s^{-1}. (b) Tafel plots of CTF, Co_2P@CTF, and Pt/C. (c) Long-term stability test of Co_2P@CTF electrode for OER in 0.5 M H_2SO_4.

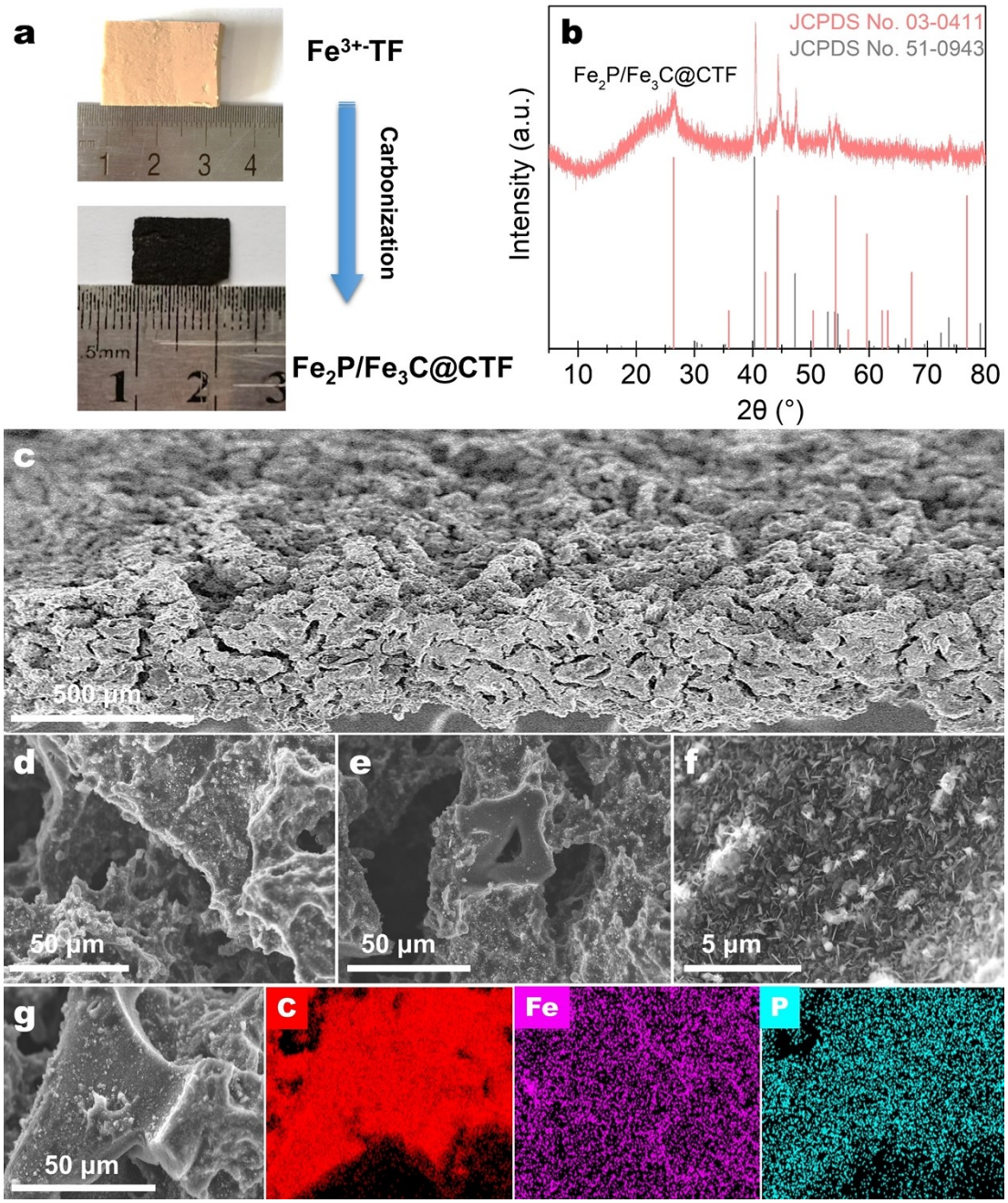

Fig. S16 (a) Photograph and (b) XRD pattern of monolithic Fe_2P/Fe_3C@CTF electrode. (c) SEM image showing the overall view of Fe_2P/Fe_3C@CTF electrode. (d) Top-view and (e) side-view SEM images of Fe_2P/Fe_3C@CTF electrode. (f) SEM image of Fe_2P/Fe_3C@CTF electrode demonstrating the uniform distribution of irregular Fe_2P/Fe_3C particles within carbon membrane matrix. (g) SEM image of Fe_2P/Fe_3C@CTF electrode and the corresponding EDX elemental mapping images (C, Fe, and P).

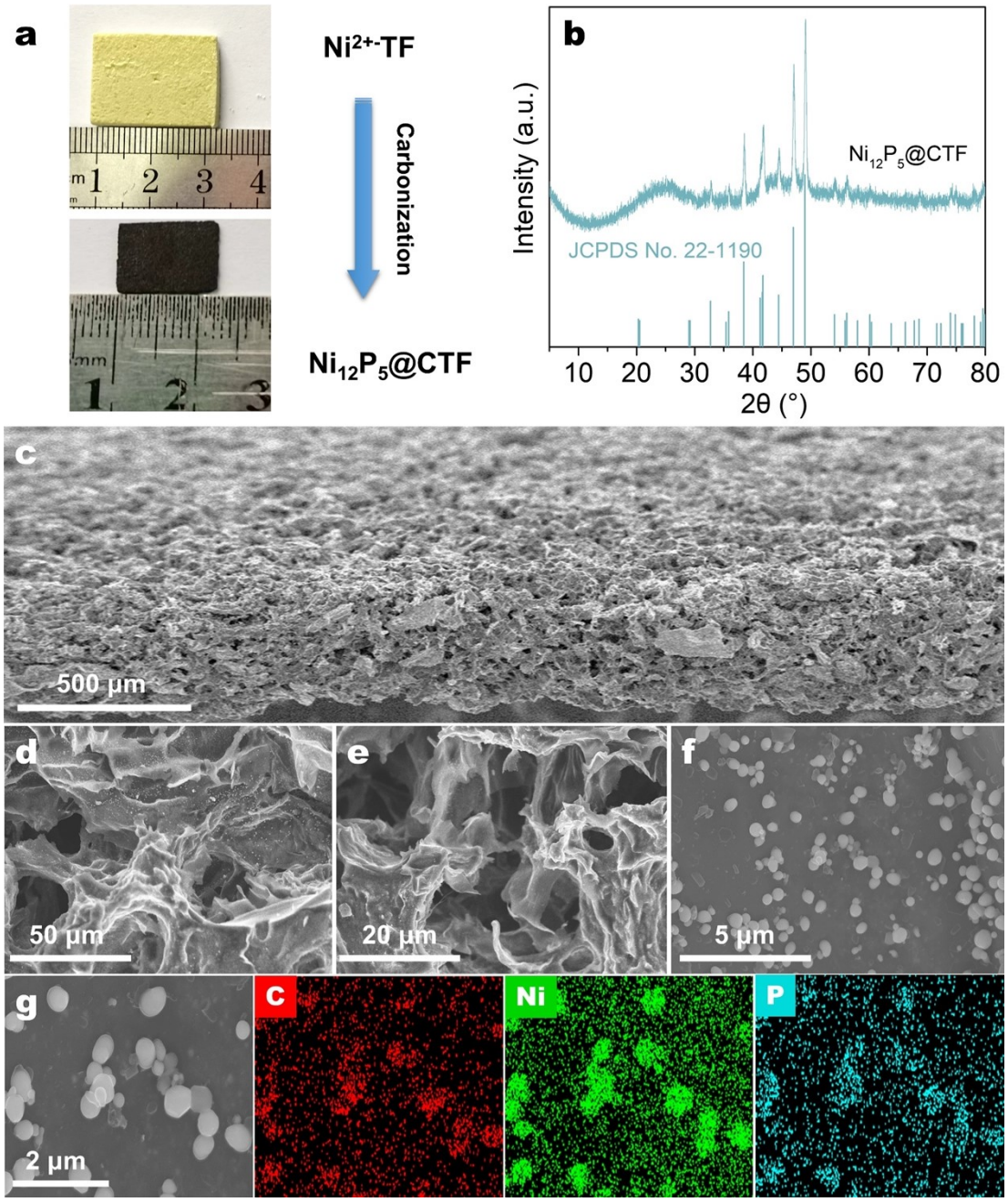

Fig. S17 (a) Photograph and (b) XRD pattern of monolithic $Ni_{12}P_5$@CTF electrode. (c) SEM image showing the overall view of $Ni_{12}P_5$@CTF electrode. (d) Top-view and (e) side-view SEM images of $Ni_{12}P_5$@CTF electrode. (f) SEM image of $Ni_{12}P_5$@CTF electrode showing the uniform distribution of $Ni_{12}P_5$ particles (~500 nm) within carbon membrane matrix. (g) SEM image of $Ni_{12}P_5$@CTF electrode and the corresponding EDX elemental mapping images (C, Ni, and P).

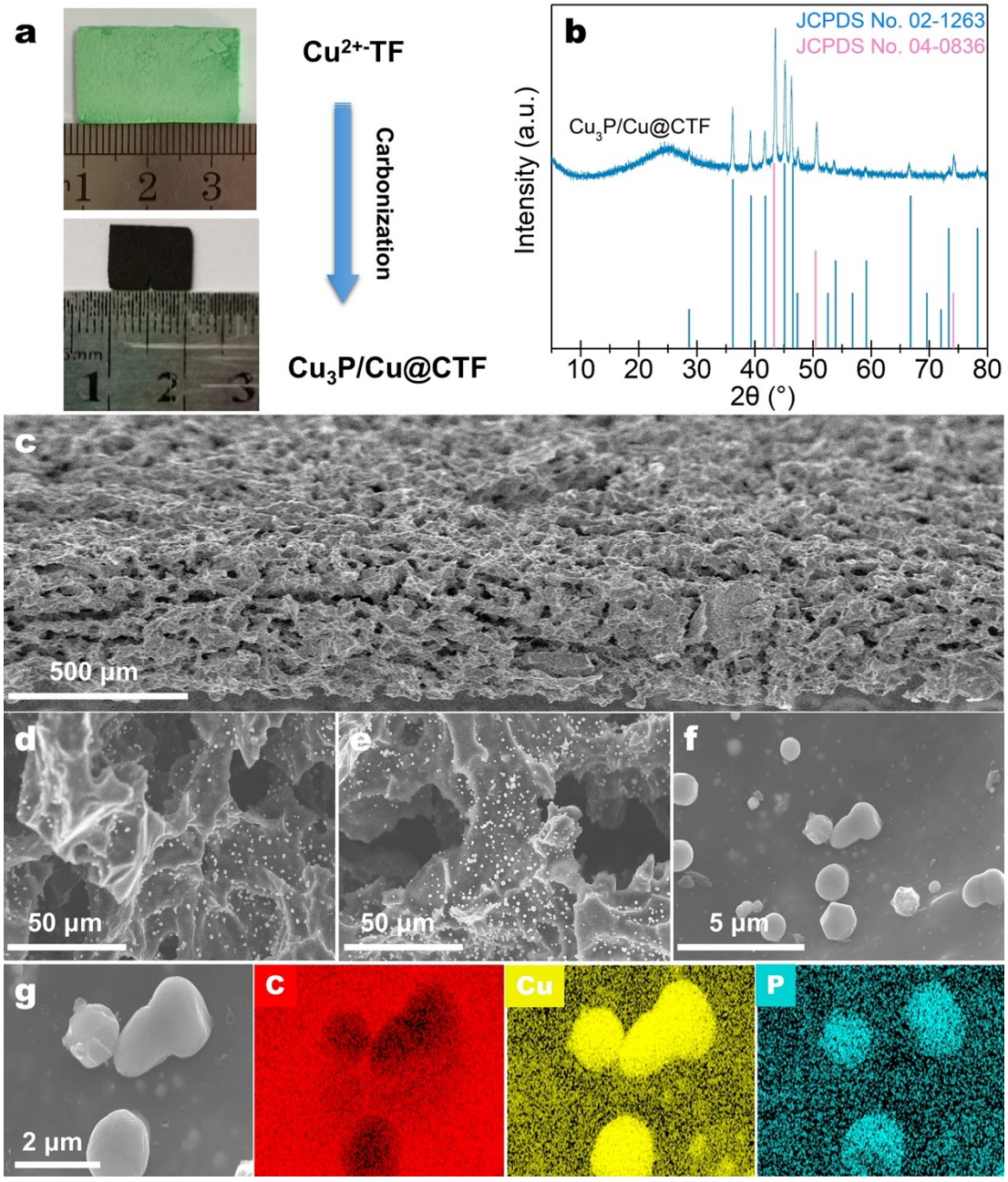

Fig. S18 (a) Photograph and (b) XRD pattern of monolithic Cu_3P/Cu@CTF electrode. (c) SEM image showing the overall view of Cu_3P/Cu@CTF electrode. (d) Top-view and (e) side-view SEM images of Cu_3P/Cu@CTF electrode. (f) SEM image of Cu_3P/Cu@CTF electrode showing the presence of large Cu_3P/Cu particles (~1 μm) on carbon membrane matrix. (g) SEM image of Cu_3P/Cu@CTF electrode and the corresponding EDX elemental mapping images (C, Cu, and P).

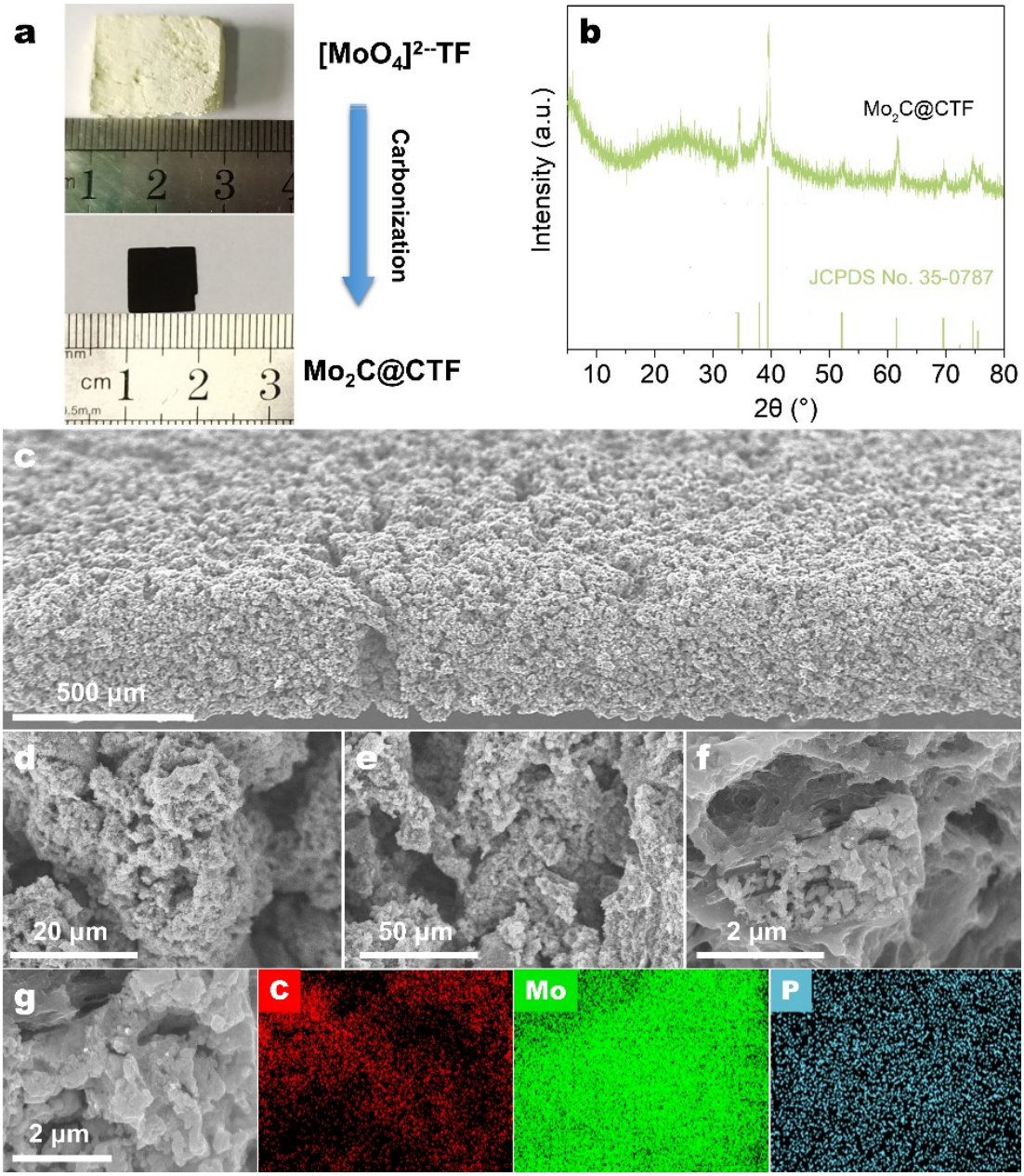

Fig. S19 (a) Photograph and (b) XRD pattern of monolithic Mo_2C@CTF electrode. (c) SEM image showing the overall view of Mo_2C@CTF electrode. (d) Top-view and (e) side-view SEM images of Mo_2C@CTF electrode. (f) High-resolution SEM image of Mo_2C@CTF electrode. (g) SEM image of Mo_2C@CTF electrode and the corresponding EDX elemental mapping images (C, Mo, and P).

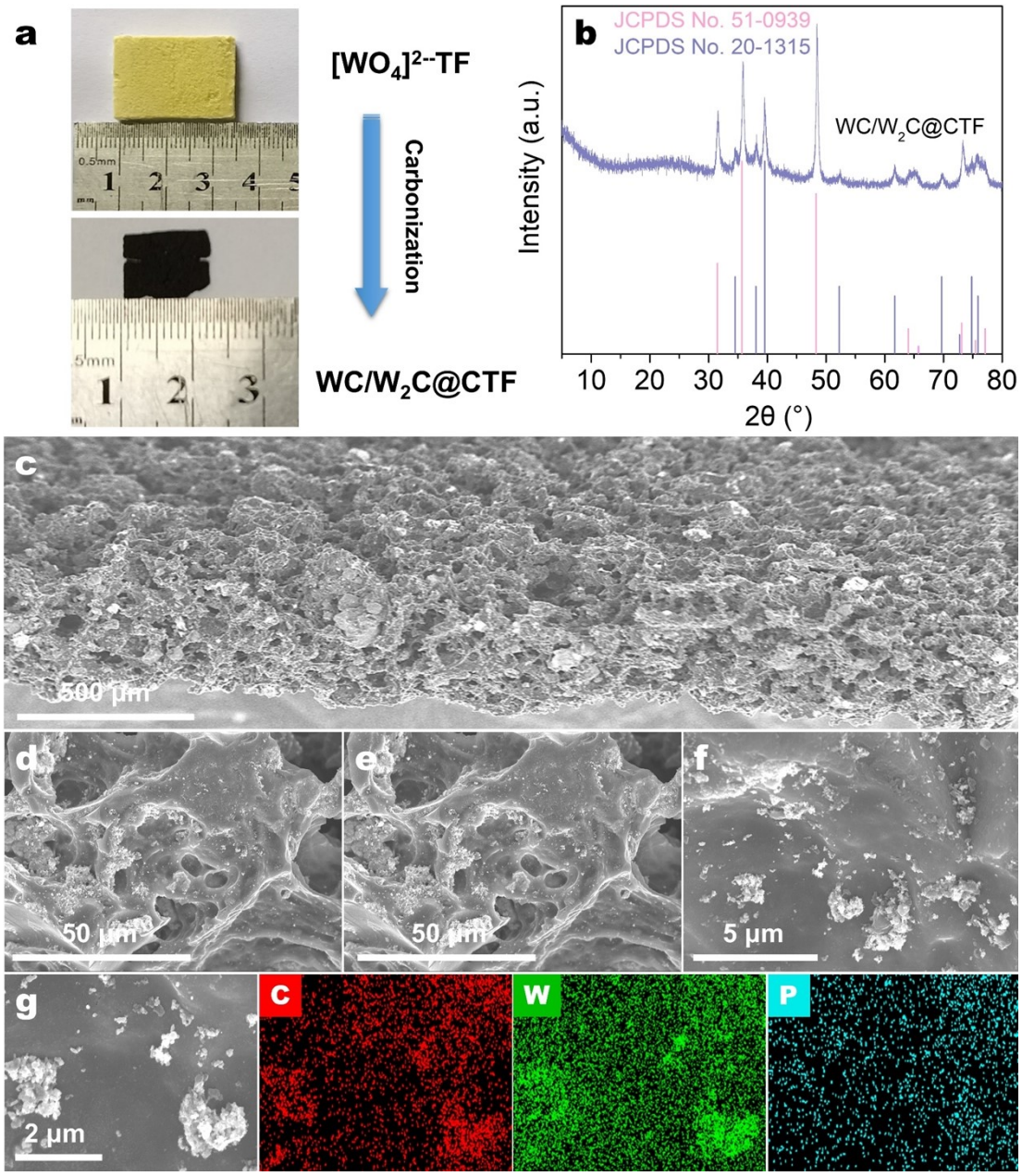

Fig. S20 (a) Photograph and (b) XRD pattern of monolithic WC/W_2C@CTF electrode. (c) SEM image showing the overall view of WC/W_2C@CTF electrode. (d) Top-view and (e) side-view SEM images of WC/W_2C@CTF electrode. (f) High-resolution SEM image of WC/W_2C@CTF electrode showing the presence of aggregated WC/W_2C particles. (g) SEM image of WC/W_2C and the corresponding EDX elemental mapping images (C, W, and P).

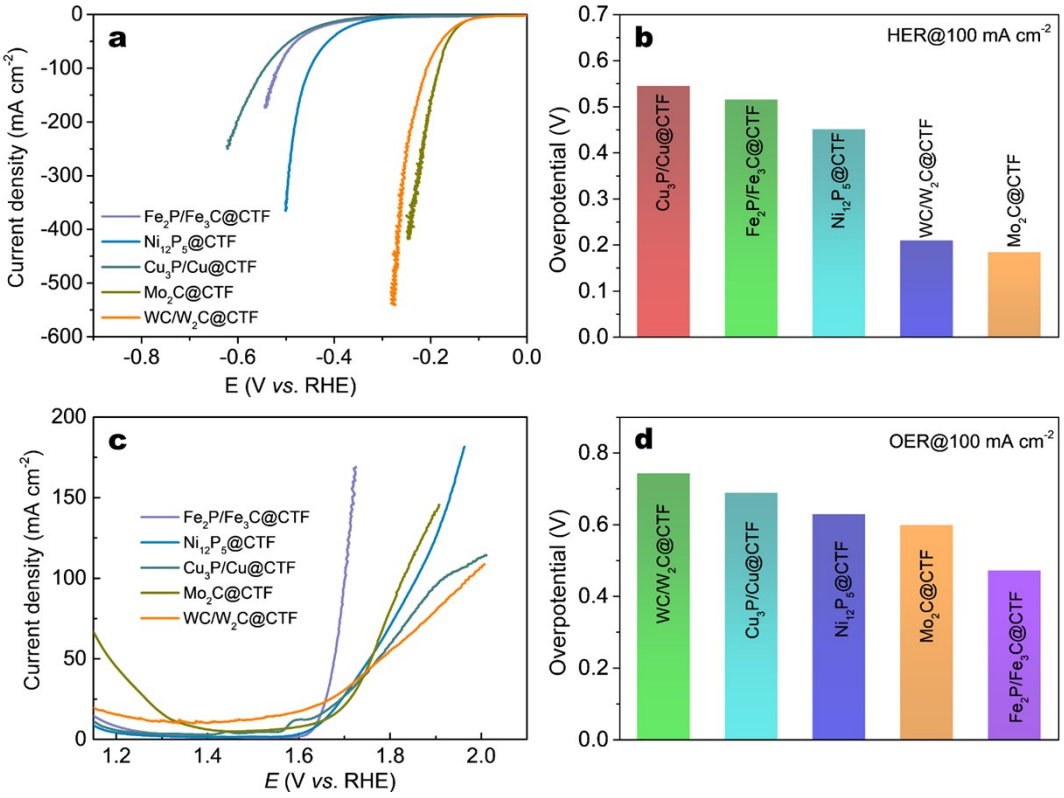

Fig. S21 (a) HER polarization curves and (b) the overpotentials at 100 mA cm^{-2} for monolithic carbon-based electrodes in 1.0 M KOH solution. (c) OER polarization curves and (d) the overpotentials at 100 mA cm^{-2} for monolithic carbon-based electrodes in 1.0 M KOH solution.